

Mehmet Bozca

Full Professor

Yildiz Technical University
Mechanical Engineering Faculty
Istanbul
Turkey**Tatjana Lazović**

Full Professor

University of Belgrade
Faculty of Mechanical Engineering
Serbia**Miloš Sedak**

Assistant Professor

University of Belgrade
Faculty of Mechanical Engineering
Serbia**Sándor Bodzás**

Associate Professor

University of Debrecen
Faculty of Engineering, Debrecen
Hungary

Numerical Analysis of Scuffing Risk in Involute Spur Gears Based on the Integral Temperature Criterion

Gear scuffing is a major concern and a critical technical challenge in gear power transmission design. This paper reviews current research and practical approaches to understanding and preventing gear scuffing, drawing on both industrial experience, available standardization and academic studies. A dedicated MATLAB-based computational code is developed to systematically analyse the influence of geometrical, operational, and lubrication parameters on flash, mass, and integral temperatures. The results show that increasing the module, tooth number, and face width positively improve scuffing resistance, while higher torque, rotational speed, and oil temperature significantly increase scuffing risk, a failure mode that can substantially reduce gear service life. The applied model and the conducted analysis have shown that the obtained results can serve as a foundation for the development of future optimization models aimed at improving gear reliability and extending service life through appropriate parameter selection and design improvement.

Keywords: Gear failure, gear scuffing, integral temperature, mass temperature, flash temperature, ISO 6336-20, ISO 6336-21, ISO 10825

1. INTRODUCTION

Gears used for power transmission are common in all areas of engineering. Their performance has a significant impact on the overall quality of the machinery, influencing reliability, energy efficiency, and environmental performance. Failures of gear teeth often propagate damage to other gear elements or connected machine components. For these reasons, gears have been extensively studied through both theoretical analyses and experimental investigations[1].

Gears are highly sensitive components of mechanical systems, and their failure can lead to substantial repair costs, prolonged downtime, and secondary damage to related machine elements [2]. The primary objective of gear design is to ensure reliable power transfer while maintaining high strength and reducing the risk of failure. As key elements of mechanical power transmission in rotating machinery, their performance and reliability are strongly governed by tribological and thermal conditions at the tooth contacts.

Gears are designed with consideration of potential failure mechanisms, and in this field, numerous standards have been established by all relevant standardization organizations, including DIN, AGMA, and ISO. Under elevated temperature, high rotational speed, heavy loading, and severe lubrication conditions, scuffing has emerged as a major concern and a critical technical challenge in gear power transmission systems. A recent review paper on gear scuffing studies [3] provides a comprehensive analysis of the scuffing phenomenon and

the state of the art in this field. This paper reviews current research and practical approaches to understanding and preventing gear scuffing, drawing on both industrial experience and academic studies. It summarizes advances in scuffing theory, experimental analysis, and the latest developments in anti-scuffing technologies. Over recent decades, extensive research on gear scuffing, including both theoretical and experimental studies, has advanced analytical approaches, numerical modeling, standardization frameworks, testing methodologies, and the development of test databases. The general conclusion can be made that, despite this progress, research in the field is still ongoing, analytical and mathematical models, numerical simulations, and experimental methods and techniques continue to be developed and refined, while artificial intelligence is increasingly being applied to practical engineering solutions.

The most influential factor affecting scuffing is the lubricant (oil) [4]. The influence of oil on the occurrence of scuffing has been analyzed from various perspectives in numerous scientific papers and practical case studies. Key parameters for evaluating gear scuffing, such as oil temperature and level, as well as surface roughness, are examined in [5,6]. Surface roughness has been recognized as a critical factor in assessing gear scuffing in [7]. Surface coatings are applied to improve surface quality and reduce friction. The effects of surface coatings on gear tooth bending fatigue, gear flank contact fatigue (pitting), abrasion, and scuffing resistance have been extensively investigated in the literature [7-11]. The influence of gear material, surface quality, and advanced lubricants on the onset of scuffing in high-speed gear contacts has been examined in [12]. According to [13], effective prevention of tribologically driven damage, such as wear and scuffing on gear flanks, depends on the proper selection of lubricant additives.

Received: December 2025, Accepted: January 2026

Correspondence to: Dr Tatjana Lazović

Faculty of Mechanical Engineering,
Kraljice Marije 16, 11120 Belgrade 35, Serbia

E-mail: tlazovic@mas.bg.ac.rs

doi: 10.5937/fme2601184B

© Faculty of Mechanical Engineering, Belgrade. All rights reserved

Dynamic loads and transient thermal elastohydrodynamic lubrication (TEHL) effects are taken into account in [14], when evaluating scuffing failure of gears. In [15], boundary and near-boundary lubrication conditions were considered during the parametric analysis of scuffing failure.

The evaluation of scuffing failure is largely influenced by the selected gear material, applied heat treatment, and the level of contact pressure on the tooth surface [16]. As shown in [17], surface finish is also an important parameter for achieving the lubrication conditions required to prevent scuffing failure. The study [18] analyzes several cases of premature gear failure using a systematic failure analysis approach. It identifies the main causes, material impurities, improper heat treatment, grinding burns, and poor lubrication, and examines how these factors lead to fatigue, spalling, and scuffing. The authors of [19] developed a spur gear model with defects, demonstrating how kinematics and lubrication affect meshing contact and stiffness. Additionally, the study [20] presents a time-varying mesh stiffness model for involute spur gears, accounting for the effects of lubrication, friction, surface roughness, and load on meshing behavior and stiffness variations along the meshing path.

Experimental research has been extensively conducted for many years in the field of gear pair failure due to scuffing, including the development of new scuffing criteria [21-23]. Power dissipation and bulk temperature during gear scuffing were analyzed in [24]. In addition, a new evaluation model based on the pressure-velocity-temperature limit was proposed in [25] to assess gear scuffing resistance. The results of these studies are based on experimental research. The authors of [26] emphasize that accurate monitoring of tooth temperature is essential for ensuring the reliable operation of gears. The study [27] presents a computational model for predicting gear tooth wear by considering temperature, friction, and dynamic meshing behaviour, highlighting uneven wear along the meshing path. In [28], an improved semi-analytical method was used to calculate flash temperature and meshing power loss under various operating conditions. Experimental findings have shown that improvements in tooth surface design lead to lower flash temperatures and reduced power losses, which enhance scuffing resistance and overall energy efficiency. By analyzing the influence of bulk (mass) temperature on gear scuffing, the authors of [29] developed a new scuffing parameter for gears lubricated with mineral-based oils and proposed that a critical gear bulk temperature exists for each lubricant viscosity grade. The paper [30] presents a finite element approach for thermodynamic analysis of gears with varying surface roughness. By incorporating 3D gear models that include tooth surface roughness, this approach allows for fast assessment of temperature increases under various machining conditions while lowering the expense of validating load-carrying capacity predictions. The study [31] presents an enhanced semi-analytical approach for calculating flash temperature on the tooth surface and investigates the influence of gear geometry, including tooth number, module, pressure angle, and helix angle, on scuffing resistance. The results

indicate that adjusting these parameters can significantly enhance the scuffing load capacity of high-speed reducer gears. The study [32] combines theoretical and experimental investigations of the scoring resistance of plane convex-concave gears by formulating generalized integral temperature criteria for various contact paths and validating them through FZG scoring tests.

Alongside experimental studies, analytical and numerical methods are being developed to assess gear anti-scuffing capacity, a critical factor for service life under high loads or speeds. Reference [33] introduces a novel analytical approach that accounts for actual lubricant film thickness and continuous heat transfer to evaluate both flash and bulk temperatures. The integral temperature method specified in ISO 6336 [34] and DIN 3990 [35] was used to analyze parameters associated with gear scuffing. Optimization in the design process [36] extends beyond weight reduction and can be applied to a wide range of performance-related criteria. In practical engineering applications, objective functions often target parameters such as structural volume, service life, cost, or failure risk. In the context of gear scuffing, the quantified influence of geometrical, operational, and lubrication parameters obtained in this study enables the formulation of optimization strategies aimed at minimizing scuffing probability while satisfying design and operating constraints. Numerous studies have shown that scuffing resistance can be significantly improved through appropriate selection and optimization of gear geometry, operating conditions, and lubrication parameters. Early analytical investigations based on the integral temperature criterion demonstrated that optimized gear geometries can substantially reduce flash temperature and scuffing risk, with good agreement between numerical predictions and experimental observations [37]. These concepts were further extended to account for micro-geometry effects, showing that profile modifications strongly influence local contact pressure and temperature distribution, and thus the initiation of scuffing [38]. Experimental studies confirmed that optimized tooth profiles, surface finishing, and operating parameters can significantly increase scuffing load capacity, particularly under severe operating conditions [39]. In parallel, recent research has increasingly employed numerical and optimization-based approaches to address scuffing as a design constraint. Multi-objective optimization frameworks have been applied to spur gears, demonstrating that inclusion of scuffing-related criteria alongside power loss, transmission error, weight, and durability leads to more reliable designs, although often at the cost of increased size or complexity [40-44]. Advanced numerical models have also been proposed to better capture the thermal and tribological mechanisms governing scuffing, including thermo-elastic heat generation, transient temperature fields, and lubrication breakdown [45,46]. Optimization studies employing evolutionary algorithms and particle swarm optimization, demonstrated that neglecting scuffing constraints can lead to designs with a high probability of surface failure, whereas their inclusion improves reliability at the cost of slightly increased volume or complexity [47-50].

Despite these advances, only a limited number of works systematically quantify the relative influence of

individual geometrical, operational, and lubrication parameters within a unified framework. Therefore, a comprehensive sensitivity-based numerical analysis, providing quantified trends and relative importance of key scuffing-related parameters, is still lacking. Such an approach can serve as a practical foundation for informed gear design decisions and for the development of future data-driven and AI-based predictive models aimed at improving gear reliability and extending service life.

This study graphically illustrates how changes in geometric characteristics, including module size, tooth number, and face width, affect the integral temperature. The influence of operating conditions, including transmitted torque and pinion rotational speed, on the integral temperature is additionally investigated. Considering lubrication parameters, the relationships between oil temperature, nominal oil viscosity, and the integral temperature are also presented graphically.

2. GEAR FAILURES

Thirty years ago, the valuable standard ISO 10825 [51] was published, dealing with the wear and failure of gears. This standard was withdrawn and revised, and in 2022 it was replaced by ISO 10825-1 [52] and the accompanying technical report ISO/TR 10825-2 [53], which provide all necessary clarifications and additional information on failure modes, as well as the theoretical background of the Standard.

Document [52] classifies, identifies, and describes gear failure modes, enabling the user to assess the degree of change in the condition and integrity of the gears compared to their initial state, immediately after manufacturing and before being put into operation. It should be noted that resolving many issues related to gear condition requires detailed investigation and analysis by both researchers and practicing engineers, which is beyond the scope of this standard.

According to [52], the most common gear failure modes are grouped into six general classes: tribological (non-fatigue) damages, fatigue damages, non-fatigue fractures, plastic deformations, manufacturing issues, and other surface damages (Figure 1).

Causes of non-fatigue tribological damage, commonly referred to as wear, may include the presence of particles suspended in the lubricant, particles embedded in the mating gear teeth, an insufficient lubricant film, or complete loss of lubrication. Wear represents the gradual removal of material from the gear tooth surface, accompanied by changes in dimensions, shape (flank profile), and surface properties of the material. The extent of wear can range from mild polishing to severe material loss, leading to tooth destruction. In certain applications, even minimal wear is unacceptable, whereas in others, a small degree of wear may be tolerated.

Fatigue damages include fatigue cracks and contact fatigue phenomena such as micropitting, macropitting, case crushing (subcase fatigue), white layer flaking, tooth flank fracture (TFF, subsurface-initiated bending fatigue), and tooth interior fatigue fracture (TIFF). Bending fatigue failures comprise tooth root fatigue fracture as well as rim, web, and hub cracks. Non-fatigue fractures may occur in brittle, ductile, or mixed

modes and include tooth root rupture, tooth end rupture, and tooth shear fracture.

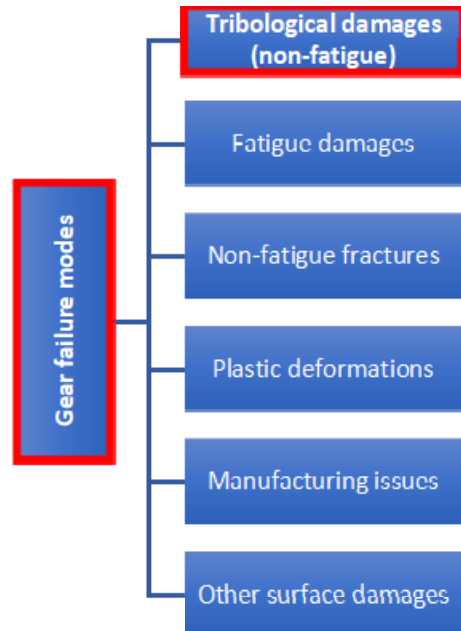


Figure 1. Classification of gear failures, according to ISO standard [52].

Plastic deformation failure modes involve indentation, brinelling, cold flow, hot flow, root fillet yielding, fracture after plastic deformation, rolling, tooth hammering, rippling, ridging burr, and interference deformation. Manufacturing-related failures may result from forging, hardening, or grinding cracks; hydrogen embrittlement and internal residual stresses; grinding burns; grinding notches; scaling; and case/core separation. In the case of forging, forging cracks can occur in the presence of oxidation. Similarly, hardening cracks may be accompanied by discoloration due to oxidation. Other surface damages include corrosion, cavitation, erosion, electrical discharge erosion, and overheating. Among other surface damages, corrosion ranks first, defined as surface degradation due to chemical and electrochemical reactions between the gear surface and its environment, and represents a very common type of damage to gear working surfaces.

The categories of tribological (non-fatigue) damages include: polishing wear, scratches, abrasive wear, scuffing, adhesive wear, fretting corrosion, and interference wear (Figure 2). Polishing typically occurs when abrasive particles become embedded in a softer mating surface, causing two-body abrasion on the harder surface. It can be intensified by chemically aggressive lubricant additives in contaminated oils. This fine-scale abrasive process gives gear teeth a bright, mirrorlike appearance.

Polishing can be classified as mild, moderate, or severe. Scratches may result from improper handling or assembly procedure, as well as from hard and abrasive particles between contacting surfaces. Such damage usually indicates inadequate cleanliness or insufficient care during gear manufacturing and/or installation.

Abrasive wear occurs when hard particles such as metallic debris, rust, or sand remove material from gear tooth surfaces. These particles may be suspended in the

lubricant or embedded in the gear teeth. The resulting scratches appear smooth, clean, and parallel to the sliding direction. Adhesive wear in gears occurs when metal surfaces come into contact under inadequate lubrication, leading to material transfer between tooth flanks. During the initial run-in period, mild adhesive wear can be beneficial, as it smooths surface irregularities and improves contact conditions, provided the load, speed, and lubrication are properly controlled [54,55]. However, if lubrication is poor or operating conditions are unfavorable, adhesive wear can become severe, causing surface damage, tooth flank profile changes, increased noise and vibration, and reduced gear life. Fretting corrosion is a localized wear that occurs when gear tooth surfaces pressed together do small cyclic movements that expel lubricant and disrupt protective oxide films. This causes direct metal-to-metal contact and adhesion between surface asperities, and even minor gear mesh interference can result in interference wear. In such cases, the gears are pressed tightly together, preventing the lubricant from maintaining a separating film between their surfaces.

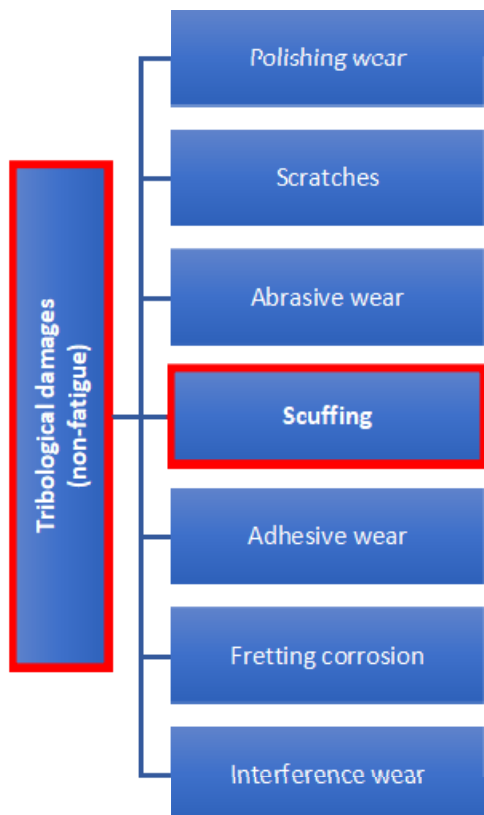


Figure 2. Tribological damages, according to the ISO standard [52].

Regardless of the large number of gear failure modes mentioned above, gear failures can generally be classified into several main categories: tooth breakage resulting from bending stress, surface pitting caused by alternating contact stress and surface fatigue, surface wear due to material removal, and scuffing resulting from high contact stress and high temperature. Preventing gear failures requires careful consideration of these potential failure mechanisms.

Tooth breakage occurs when a whole tooth or a portion of it fractures, typically due to sudden static

overload or alternating loads. Gear teeth typically experience cyclic loading, and if the stress level repeatedly or occasionally surpasses the gear's fatigue strength, fatigue failure can occur [56,57]. Fatigue failure generally evolves in three stages: crack initiation at regions of high stress concentration, subsequent crack propagation under cyclic loading, and final sudden fracture once the remaining load-bearing section can no longer sustain the applied load. Crack initiation usually occurs at or near the surface, where defects such as scratches, pits, geometric discontinuities, or material inhomogeneities are present. These features promote localized plastic deformation and slip, which trigger crack formation, often after a certain period of service rather than immediately at load application [58, 59].

Pitting represents a form of surface fatigue manifested as the formation of very small local depressions on surfaces subjected to repeated rolling and sliding contact. The pitting resistance or durability of a gear pair refers to its ability to operate for a sufficiently long period without the occurrence of such surface damage [60]. Pitting on tooth flanks is characterized by the development of pinholes and progressive spalling on the surface, typically occurring below the pitch circle, and is a common indicator of material fatigue. Surface cracks caused by sliding/rolling stress or subsurface cracks induced by high shear stress beneath the flank surface can initiate pitting failure. The Hertzian stress theory is applied to evaluate the load-carrying capacity against pitting and to determine the surface stress [56,61]. Wear occurs when material is removed from the mating surfaces under thin-film lubrication during each load cycle. It is a progressive form of failure that typically develops at low pitch-line velocities, where asperity interactions are more likely.

Scuffing is a sudden, non-fatigue failure mode representing a severe form of adhesion, involving either material transfer between gear tooth surfaces or material loss due to lubricant film breakdown, welding, and tearing. It usually appears away from the pitch line as narrow or wide bands oriented in the sliding direction, and in areas of high stress concentration, it may form patches. Scuffed regions are matte and discolored, and under a microscope, the surfaces appear rough, torn, and plastically deformed, with altered metallic structure and hardness compared to undamaged flanks. Standard [52] distinguishes between hot and cold scuffing and classifies it as mild, moderate, or severe, with each category described and illustrated in detail. In its most severe form, scuffing involves local adhesion or micro-welding of gear tooth surfaces caused by the failure of the lubricating film under extreme thermal and pressure conditions. While this phenomenon commonly appears at high surface velocities, it can also occur at lower sliding speeds provided that the contact stresses are sufficiently elevated [34,62].

3. FRICTION AND LUBRICATION CONDITIONS

Gears run under three main friction conditions: boundary friction, mixed friction and fluid friction, as shown in Figure 3.

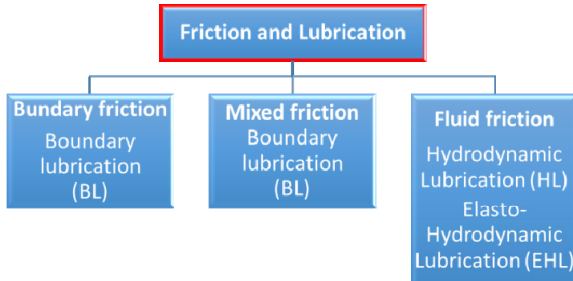


Figure 3. Friction and lubrication classifications.

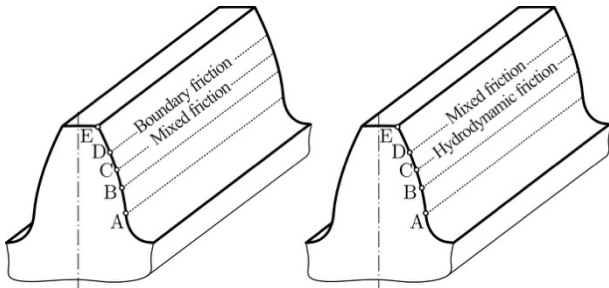


Figure 4. Scuffed gear surface

Point A marks the initial contact, B the internal single contact, C the pitch point, D the external single contact, and E the final contact. Sliding speed is highest at the beginning (A) and end (E) of engagement, occurring at the tooth root or tip, and is zero at the pitch point C. Lubrication is most effective near the pitch point, while the tooth tips experience less favorable conditions due to meshing impacts and elevated temperatures from higher sliding speeds [56]. Scuffing failure results from a combination of physical and, especially, chemical processes. The physical aspects are explained by elasto-hydrodynamic lubrication theory, whereas the chemical reactions occur in extremely thin layers under high pressure and are highly complex. Two distinct types of lubricant films can be identified: the elasto-hydrodynamic lubrication (EHL) film and the chemical protective film, which forms due to reactions between rim zone materials and lubricant additives [56]. Gear wheels typically operate within the mixed friction regime, although hydrodynamic lubrication occupies a larger portion of the contact path compared to mixed and boundary friction [56]. Scuffing is initiated when the protective chemical film on the tooth flank breaks down. The film's durability is influenced by the tooth flank temperature, while the stress on the film is governed by Hertzian contact stress. Increasing the lubricant viscosity, which thickens the film, can help mitigate scuffing failure [56].

The effective parameters for scuffing failure are shown in Figure 5.

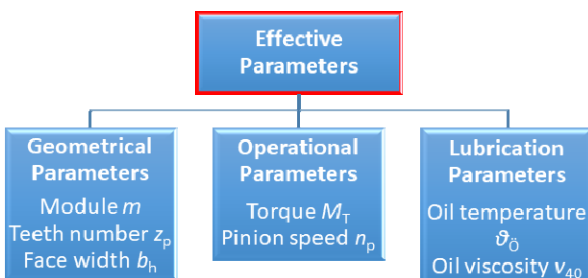


Figure 5. Effective parameters for scuffing failure

Scuffing failure can be assessed by geometrical parameters such as the module, pinion tooth number, and face width, by operational parameters including the transmitted torque and pinion rotational speed, as well as by lubrication parameters such as oil temperature and the nominal oil viscosity at 40 °C.

4. CALCULATING THE SCUFFING LOAD CAPACITY

According to ISO and DIN guidelines[34,35,62,63], scuffing evaluation is based on the premise that excessive contact stresses combined with sliding motion generate elevated surface temperatures, which can ultimately lead to the collapse of the lubricating film. To address this mechanism, the standards introduce two distinct temperature-based calculation concepts. One approach evaluates scuffing by determining an overall surface temperature expressed as a weighted average along the entire tooth contact trajectory, commonly referred to as the integral temperature method. An alternative method emphasizes localized thermal effects by computing transient contact temperatures at specific points along the contact path, known as the flash temperature method. In the present study, however, scuffing load-carrying capacity is evaluated using the integral surface temperature approach.

The assessment of scuffing using the integral temperature criterion relies on the premise that scuffing is likely when the mean contact temperature, averaged along the entire contact path, reaches or exceeds a specified threshold known as the permissible integral temperature. This integral temperature is defined as the combination of the bulk temperature and a weighted average of the flash temperature contributions accumulated along the contact path. The probability of scuffing is determined by comparing the calculated integral temperature with the corresponding permissible value. The permissible integral temperature is defined based on experimental tests of gear lubricants for scuffing resistance or on the analysis of gears that have failed from scuffing in service.

The integral temperature is calculated in accordance with ISO and DIN formulations[34,35,62,63]:

$$\vartheta_{\text{int}} = \vartheta_M + C_2 \cdot \vartheta_{\text{fla}int} \leq \vartheta_{\text{int}p} \quad (1)$$

where: ϑ_M (°C) is the mass temperature of the tooth surface just before loading; C_2 is an experimentally determined weighting factor, typically taken as 1.5; $\vartheta_{\text{fla}int}$ (°C) is a average flash integral temperature; $\vartheta_{\text{int}p}$ (°C) is a permissible integral temperature.

The mass temperature is calculated using the expressions provided in [34,35,62,63]:

$$\vartheta_M = X_S \cdot (\vartheta_0 + C_1 \cdot \vartheta_{\text{fla}int}) \quad (2)$$

where: X_S is the lubrication factor (for splash lubrication, X_S is taken as 1, while X_S is 1.2 for injection lubrication and X_S is 0.2 for gears running fully in oil); ϑ_0 (°C) is the temperature of the lubricating oil before tooth engagement; C_1 is an experimental weighting factor, assumed to be 0.7; $\vartheta_{\text{fla}int}$ (°C) is the average flash integral temperature.

The average flash integral temperature can be determined using the following equation [34,35,62,63]:

$$\vartheta_{\text{flaint}} = \vartheta_{\text{flaE}} \cdot X_e \quad (3)$$

where: ϑ_{flaE} (°C) is the flash temperature at the pinion's engagement point E; X_e is the contact ratio factor.

The flash temperature at point E is calculated using the formula [34,35,62,63]:

$$\vartheta_{\text{flaE}} = K \cdot \mu_{mc} \cdot \frac{w_n |v_{t1} - v_{t2}|}{\sqrt{2 \cdot b_h} (B_{M1} \cdot \sqrt{v_{t1}} + B_{M2} \cdot \sqrt{v_{t2}})} \quad (4)$$

where: $K = 1.11$ is empirical factor; μ_{mc} is the average coefficient of friction; w_n (N/mm) is the line load in the normal direction; $v_{t1,2}$ (m/s) are the tangential velocities of radii 1 and 2; b_h is the face width, and $B_{M1,2}$ are the thermal contact coefficients of radii 1 and 2.

The thermal contact coefficient is calculated as follows [34,35,62,63]:

$$B_M = \sqrt{(\lambda_M \cdot c_v)} \quad (5)$$

where: $\lambda = 50$ N/sK is heat conductivity; $c_v = 3,8$ N/mm²K is the specific heat capacity per unit volume.

The permissible integral temperature is determined using the expressions given in [34,35,62,63]:

$$S_{\text{int}P} = \frac{\vartheta_{\text{int}S}}{S_{\text{S min}}} \quad (6)$$

$$\vartheta_{\text{int}S} \approx \vartheta_{MT} + X_{\text{WrelT}} \cdot C_2 \cdot \vartheta_{\text{flaintT}} \quad (7)$$

where: $S_{\text{S min}}$ is the minimum scuffing safety factor; ϑ_{MT} (°C) is the mass temperature depending on the pinion torque; X_{WrelT} is the relative structure factor; $\vartheta_{\text{flaintT}}$ (°C) is the average flash temperature; the subscript T denotes values obtained from measurements during the scuffing test on the test bench.

The mass temperature and measured average flash integral temperature are calculated according to [34,35,62,63]:

$$\vartheta_{MT} = 80 + 0.23 \cdot M_{T1T} \quad (8)$$

$$\vartheta_{\text{flaintT}} = 0.08 \cdot M_{T1T}^{1,2} \cdot \left(\frac{100}{v_{40}} \right)^{v_{40}^{-0.4}} \quad (9)$$

where: M_{T1T} (Nm) is the pinion torque; v_{40} (mm²/s) is the nominal kinematic viscosity.

The scuffing safety factor, calculated using the integral temperature method, is determined according to [34,35,62,63]:

$$S_{\text{int}S} = \frac{\vartheta_{\text{int}S}}{\vartheta_{\text{int}}} \geq S_{\text{S min}} \quad (10)$$

Three conditions describe the occurrence of scuffing failure:

1. If $S_{\text{int}S} > 1.0$ the gears do not experience scuffing.
2. If $S_{\text{int}S} = 1.0$ the gears are at the scuffing limit.
3. If $S_{\text{int}S} < 1.0$ the gears experience scuffing.

5. NUMERICAL ANALYSIS

In this numerical study, the MATLAB program is employed to simulate the effects of the assumed geometrical, operational, and lubrication parameters on the integral temperature. A flowchart of the calculation algorithm is presented in Figure 6.

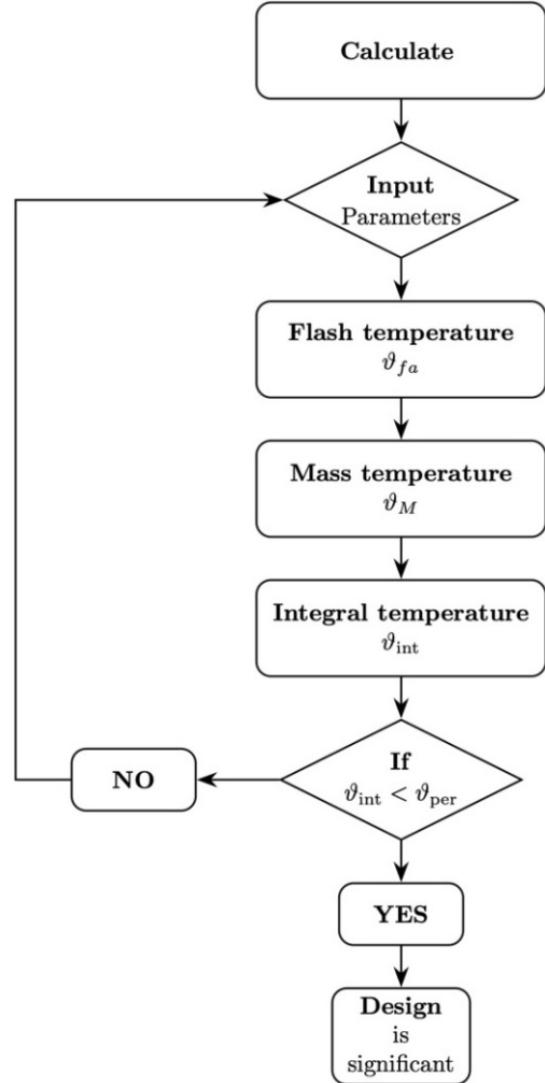


Figure 6. Flow chart of the scuffing calculation for involute spur gears

For the simulation of the effective parameters on scuffing failure, module m is 9 mm, the number of pinion teeth z_p is 17, the face width b_h is 60 mm, the pinion speed n_p is 1300 rpm, the transmitted torque M_{T1T} is 372 Nm, the oil temperature ϑ_0 is 100 °C, the lubricant kinematic viscosity at 40 °C v_{40} is 220 mm²/s, the lubricant factor X_S is 1.0, and the friction coefficient μ is 0.073.

Integral temperatures are simulated by systematically varying the key parameters associated with scuffing failure, including geometric, operating, and lubrication-related factors.

The effects of the module on flash temperature, mass temperature and integral temperature are presented in Table 1.

Figure 7 illustrates the simulated variation of the flash temperature as a function of the module. The re-

sults indicate that an increase in the module leads to a reduction in flash temperature. The same figure shows the plot of module versus the change in the mass temperature, indicating that an increase in the module leads to a reduction in the mass temperature. Figure 7 also depicts the change in the integral temperature as a function of module, showing that higher module values result in lower integral temperatures.

Table 1. Relationship between module and scuffing temperatures

No	Module	Flash	Mass	Integral
		temperature	temperature	temperature
	m [mm]	ϑ_{fla} [°C]	ϑ_M [°C]	ϑ_{int} [°C]
2	2	257.664	280.365	666.900
3	3	196.562	237.593	532.400
4	4	166.011	216.207	465.200
5	5	147.680	203.376	424.900
6	6	135.459	194.822	398.000
7	7	126.731	188.711	378.800
8	8	120.184	184.129	364.400
9	9	115.092	180.564	353.200
10	10	111.019	177.713	344.200

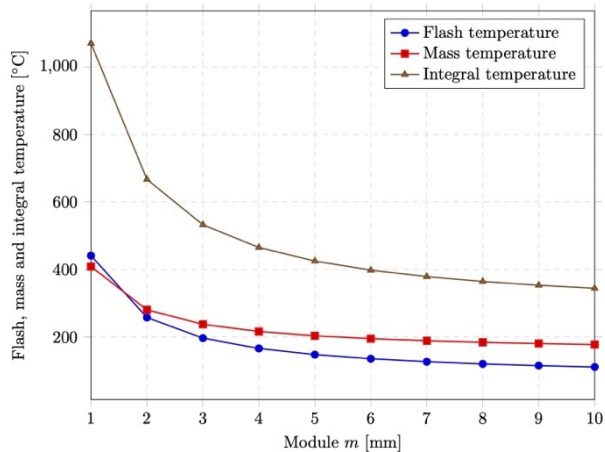


Figure 7. Flash, mass and integral temperatures vs. module

Gear pairs characterized by smaller normal modules show a pronounced sensitivity to thermal effects. As the normal module increases from 2 to 10 mm (Table 1), a significant decrease in all characteristic temperatures is observed. Specifically, the flash temperature is reduced from 257.664°C to 111.019°C, while the mass temperature decreases from 280.356°C to 177.713°C. A similar trend is evident for the integral temperature, which declines from 666.900°C to 344.200°C, as shown in Figure 7. These results can be attributed to the enlargement of the contact area at higher module values, leading to lower contact pressures and reduced frictional heat generation.

The effects of tooth number on flash temperature, mass temperature and integral temperature are presented in Table 2.

The effect of different pinion tooth numbers on the flash, mass, and integral temperature is simulated and shown in Figure 8. Simulations show that increasing the number of teeth reduces the flash temperature. A similar decreasing trend is observed for both the mass and the integral temperature.

Table 2. Flash, mass and integral temperature depending on tooth number

No	Tooth number	Flash temperature	Mass temperature	Integral temperature
	z_p	ϑ_{fla} [°C]	ϑ_M [°C]	ϑ_{int} [°C]
1	14	123.821	186.675	372.406
2	15	120.523	184.366	365.151
3	16	117.638	182.347	358.804
4	17	115.092	180.564	353.203
5	18	112.829	178.980	348.224
6	19	110.804	177.563	343.769
7	20	108.982	176.287	339.760
8	21	107.333	175.133	336.133
9	22	105.834	174.084	332.835
10	23	104.466	173.126	329.824

An increase in the pinion tooth number from 14 to 34 also contributes to a reduction in thermal loading, as shown in Table 2. The flash temperature decreases from 123.821°C to 104.466°C, accompanied by a reduction in mass temperature from 186.675°C to 173.126°C. Likewise, the integral temperature is lowered from 372.406°C to 329.824°C (Figure 8). A larger tooth number promotes a more favorable load sharing mechanism, thereby diminishing local contact stresses and associated heat production.

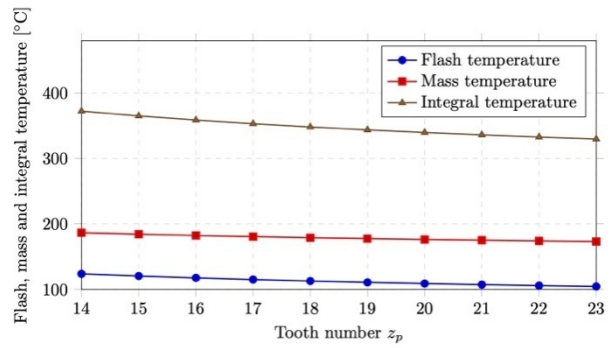


Figure 8. Flash, mass and integral temperatures vs. the number of pinion teeth

The effects of face width on flash temperature, mass temperature and integral temperature are presented in Table 3.

Table 3. Relationship between face width and scuffing temperatures

No	Face width	Flash temperature	Mass temperature	Integral temperature
	b_h [mm]	ϑ_{fla} [°C]	ϑ_M [°C]	ϑ_{int} [°C]
1	20	74.569	152.198	264.052
2	25	74.509	152.156	263.919
3	30	74.473	152.131	263.839
4	35	74.449	152.114	263.787
5	40	74.432	152.103	263.751
6	45	74.420	152.094	263.724
7	50	74.411	152.088	263.704
8	55	74.404	152.083	263.688
9	60	74.398	152.079	263.676
10	65	74.393	152.075	263.665

By varying the face width, the change in the flash temperature, mass temperature, and integral temperature is simulated and presented in Figure 9. As the face

width increases, the flash temperature decreases, and both the mass temperature and integral temperature decrease. The effect of increasing face width from 20 to 65 mm is shown in Table 3. Flash temperature slightly decreases from 74.569°C to 74.393°C, mass temperature from 152.156°C to 152.075°C, and integral temperature from 264.052°C to 263.665°C (Figure 9). The limited effect of face width suggests that, beyond a certain point, further widening does not significantly influence load distribution or heat generation.

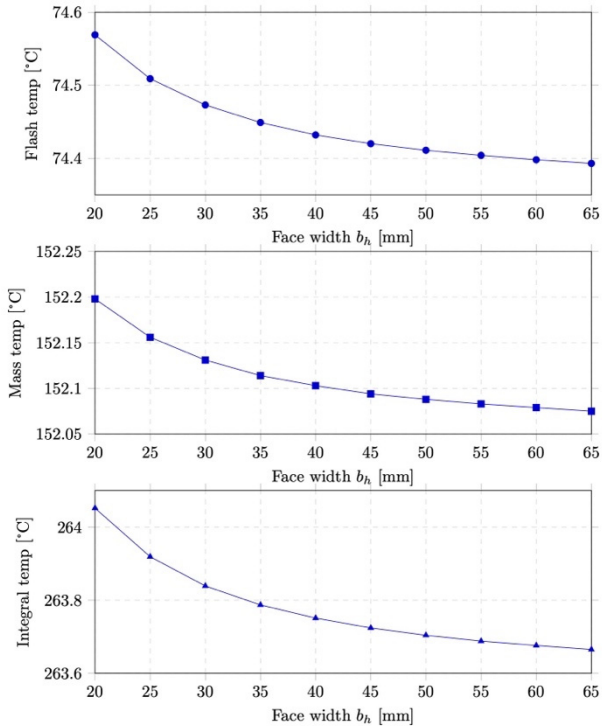


Figure 9 Temperatures vs. face width.

Table 4. Relationship between torque and scuffing temperatures

No	Torque	Flash temperature	Mass temperature	Integral temperature
	M_T [N·m]	ϑ_{fla} [°C]	ϑ_M [°C]	ϑ_{int} [°C]
1	200	96.258	167.380	311.767
2	400	118.158	182.711	359.948
3	600	140.059	198.041	408.129
4	800	161.959	213.371	456.310
5	1000	183.859	228.702	504.491
6	1200	205.760	244.032	552.672
7	1400	227.660	259.362	600.852
8	1600	249.561	274.692	649.033
9	1800	271.461	290.023	697.214
10	2000	293.362	305.353	745.395

The effects of transmitted torque on flash temperature, mass temperature and integral temperature are presented in Table 4. Simulations were carried out by changing the transmitted torque. The effects on flash, mass, and integral temperature are shown in Figure 10. From Figure 10, it is observed that increasing the torque results in an increase in the flash temperature. Furthermore, the same behaviour is observed with the mass and integral temperature, where it is obvious that the increase in torque results in an increase in these

parameter values. Increasing the transmitted torque from 200 to 2000 Nm results in substantial increases in temperatures (Table 4). The flash temperature increases from 96.258°C to 293.362°C, the mass temperature rises from 167.380°C to 305.353°C, and the integral temperature reaches 745.395°C from an initial value of 311.767°C (Figure 10). A tenfold increase in torque leads to approximately a threefold increase in flash temperature, a 1.8-fold rise in mass temperature, and a 2.4-fold increase in integral temperature. Higher torque elevates contact stresses, increasing frictional heating and the risk of scuffing.

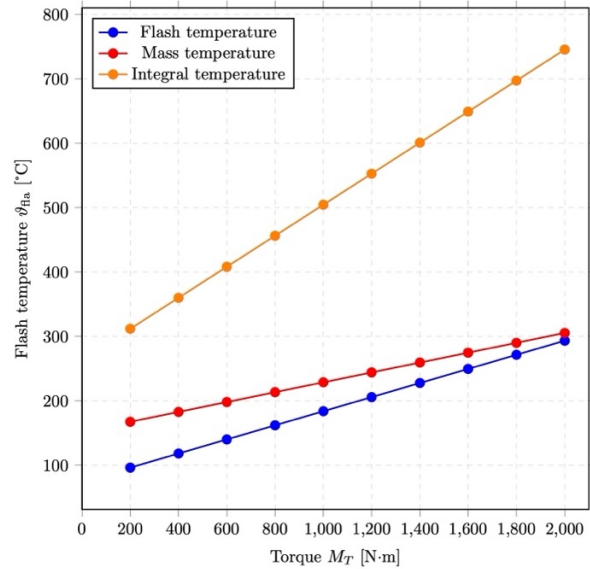


Figure 10 Flash temperature vs. transmitted torque

The effects of pinion speed on the mass temperature are shown in Table 5. The flash temperature depends on the tangential velocity components defined in Eq. (4). Although these velocities vary with rotational speed, the selected speed range is intentionally narrow, resulting in negligible variations of tangential velocity. As the tangential component of velocity is assumed to be constant, it results in a constant flash temperature. The flash temperature is 74.40°C, and the integral temperature is 263.68°C. Higher pinion speeds result in increased mass temperature (Figure 11). Higher pinion speeds, ranging from 1000 to 1900 rpm, lead to increased mass temperatures from 176.01°C to 333.36°C (Table 5, Figure 11). The elevated sliding velocity at higher speeds intensifies frictional heat generation, which may compromise scuffing resistance if not managed properly.

Table 5. Relationship between pinion speed and scuffing temperatures

No	Pinion speed	Mass temperature
	n_p [rpm]	ϑ_M [°C]
1	1000	176.01
2	1100	193.49
3	1200	210.98
4	1300	228.46
5	1400	245.94
6	1500	263.43
7	1600	280.91
8	1700	298.39
9	1800	315.88
10	1900	333.36

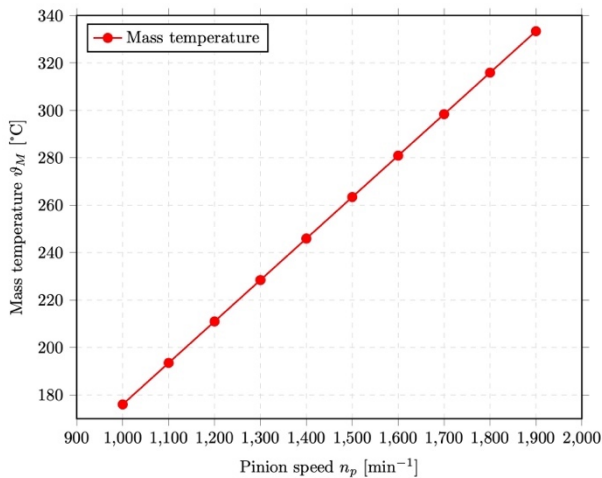


Figure 11. Mass temperature vs. pinion speed.

The effects of oil temperature on flash temperature, mass temperature and integral temperature are presented in Table 6. The flash temperature is calculated according to Eq. (3) using a fixed number of revolutions, which inherently leads to a constant flash temperature value of 74.398°C.

Table 6. Relationship between lubricant temperature and scuffing temperatures

No	Lubricant temperature	Mass temperature	Integral temperature	
		ϑ_0 [°C]	ϑ_M [°C]	ϑ_{int} [°C]
1	50		102.079	213.676
2	60		112.079	223.676
3	70		122.079	233.676
4	80		132.079	243.676
5	90		142.079	253.676
6	100		152.079	263.676
7	110		162.079	273.676
8	120		172.079	283.676
9	130		182.079	293.676
10	140		192.079	303.676

Simulations were carried out by varying the oil temperature. The resulting changes in the mass temperature are illustrated in Figure 12. An increase in oil temperature causes the mass temperature to rise. The figure also shows the corresponding changes in the integral temperature. It can be observed that higher oil temperatures lead to an increase in integral temperature. Lubricant inlet temperature further affects the thermal state of the gear pair. An increase in oil temperature from 50°C to 100°C causes the mass temperature to rise from 102.079°C to 192.079°C, while the integral temperature increases from 213.676°C to 303.676°C (Figure 12). An increase in oil temperature by 2.8 times causes an increase in the mass temperature by 1.9 times and an increase in the integral temperature by 1.4 times. Higher lubricant temperatures reduce viscosity, which can slightly increase surface heating due to a thinner lubrication film.

The effects of nominal viscosity on flash temperature are presented in Table 7. The mass temperature is calculated according to Eqs. (2)-(4) and depends on the flash temperature defined by Eq. (3). It does not depend on the total flash temperature given in Eq. (9).

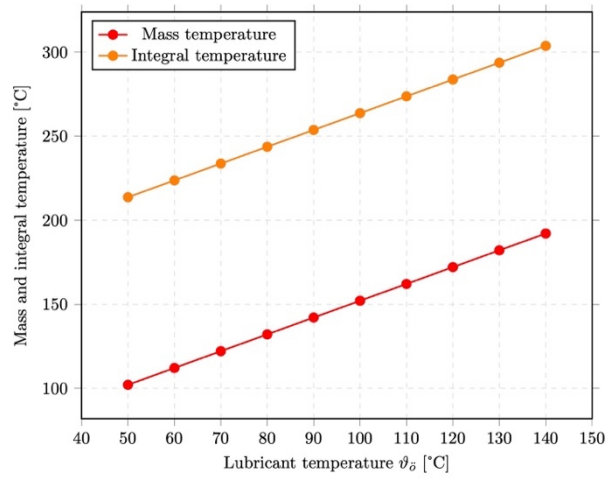


Figure 12. Mass and integral temperatures vs. lubricant temperature

Table 7. Relationship between nominal viscosity and scuffing temperatures

No	Nominal viscosity	Flash integral temperature
	ν_{40} [mm²/s]	ϑ_{plain} [°C]
1	200	89.451
2	220	88.746
3	240	88.163
4	260	87.673
5	280	87.256
6	300	86.899
7	320	86.590
8	340	86.320
9	360	86.084
10	380	85.876

The mass temperature is 152.079°C and the integral temperature is 263.676°C. The results shown in Figure 13 indicate that increasing of ν_{40} leads to a decrease in flash integral temperature. Increasing oil viscosity from 200 to 400 mm²/s reduces the flash integral temperature from 89.451°C to 85.876°C (Figure 13). Higher viscosity improves the lubricant film, reducing frictional heating and enhancing scuffing resistance.

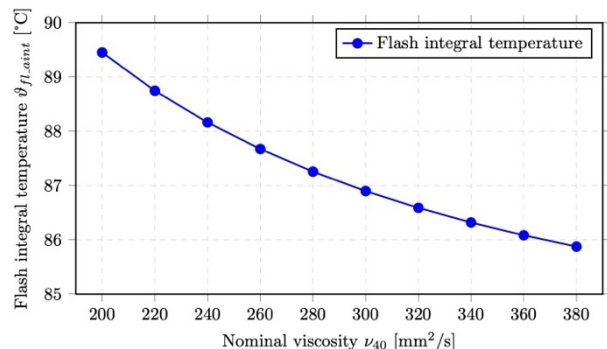


Figure 13. Flash integral temperature vs. nominal kinematic viscosity

6. RESULTS AND DISCUSSION

Table 8 compares the effectiveness of different parameters on scuffing resistance. Parameters are classified as having either a positive or a negative influence. Overall, geometric factors such as module and tooth number generally enhance scuffing resistance, while

operational factors like torque and speed may increase the risk of scuffing if not properly controlled. Lubrication parameters, including oil temperature and viscosity, play a crucial role in maintaining safe operating conditions.

Table 8. Qualitative Influence of Gear and Operating Parameters on Scuffing Resistance

Parameters		Strongly Positive effect	Slightly Positive effect	Strongly Negative effect	Slightly Negative effect	Scuffing resistance
Module m [mm]	↗	★				↗
Teeth number z_p	↗		★			↗
Face width b_h [mm]	↗		★			↗
Torque M_T [Nm]	↗			★★		↘
Speed n_p [min ⁻¹]	↗			★★		↘
Oil temperature [°C]	↗			★		↘
Kinematic viscosity ν_{40} [mm ² /s]	↗		★			↗

From previous observations, it can be concluded:

- larger module, higher tooth number, and wider face width positively improve resistance to scuffing failure in gears.
- selecting gears with larger geometric dimensions is essential not only to prevent tooth breakage and pitting but also to minimize the risk of scuffing under operational loads.

Considering operational parameters, increasing the transmitted torque strongly elevates flash, mass, and integral temperatures. Similarly, a higher pinion speed leads to a significant increase in the mass temperature. Therefore:

- higher torque and increased rotational speed negatively affect gear scuffing resistance.
- gears with larger geometries should be selected to ensure safe operation, since operational conditions often cannot be modified.

Regarding lubrication parameters, higher oil temperature strongly increases both mass and integral temperatures, while a higher nominal kinematic viscosity slightly decreases the integral temperature. Accordingly:

- increased nominal kinematic viscosity improves scuffing resistance.
- using lubricants with elevated viscosity can effectively reduce the probability of scuffing failure in gears.

The analysis of the impact of various gear parameters on gear scuffing under elevated contact temperatures allows for the formalization of scuffing risk as a quantifiable constraint function within future design and optimization models. This enables the appropriate sensitivity analysis, which enables researchers and designers to systematically explore solution spaces to

identify configurations that maximize reliability and minimize the potential for scuffing failure. Additionally, the sensitivity analysis helps in formulating the appropriate solution space boundaries, which is the crucial step in formulating complex constrained optimization problems, which can be considered as an additional contribution of this work.

As is well known, gear material and heat treatment significantly influence scuffing resistance. Therefore, these factors should be taken into account when analyzing the scuffing phenomenon and all relevant influencing parameters, both in the selection of materials and hardening methods [64,65], and in the process of their regeneration [66,67]. A limitation of the present analysis is that material properties, hardness, and heat treatment conditions were not considered, which could be addressed in future studies. Nevertheless, the obtained results offer a solid basis for developing a first iteration of predictive models for scuffing, accounting for geometric and kinematic parameters of the gear transmission as well as appropriate operating conditions. This work, therefore, serves as a practical reference for engineers aiming to improve gear reliability and extend service life through informed parameter selection and design optimization. The present study is based exclusively on numerical simulations. Attempts were made to identify comprehensive, systematised future experimental data covering the wide range of geometrical, operational, and lubrication parameters considered in this analysis. The assessment deliberately relies on the recommendations and formulations provided in the relevant ISO standards, which are considered well-established, validated, and justified for the analytical evaluation of scuffing risk. The numerical analysis presented here, along with the identified dependencies, trends, and sensitivities of temperature-related scuffing parameters, serves as a foundational step toward the development of an optimization model. Such models typically require well-defined constraints and initial assumptions before being progressively expanded to include additional influencing factors. The actual optimization results would be the subject of potential subsequent work.

7. CONCLUSIONS

This study presents a comprehensive numerical assessment of gear scuffing risk based on the integral temperature criterion. A dedicated MATLAB-based computational code was developed to systematically analyze the influence of geometrical, operational, and lubrication parameters on flash, mass, and integral temperatures. The main scientific contributions are:

- the implementation of a numerical methodology for scuffing assessment that enables rapid and consistent evaluation of scuffing risk,
- the definition of practical parameter ranges for gear geometry in relation to lubricant viscosity and operating temperature, and
- the possibility of early identification of geometric and operating conditions associated with a high scuffing risk, which directly affects gear service life.

The results confirm that increasing the module, tooth number, and face width improves scuffing resistance, while higher torque, rotational speed, and oil temperature significantly increase scuffing risk, a failure mode that can significantly reduce gear service life. Higher lubricant viscosity contributes positively by improving lubrication conditions and reducing thermal loading. Quantifying the effects of geometrical, operational, and lubrication parameters provides essential guidance for design engineers when selecting gear dimensions and operating conditions. Moreover, the results can be used to optimize gear design by identifying the most favourable combination of parameters that minimizes the probability of scuffing in a justified and reliable manner. Also, obtained results form a solid basis for future extensions toward predictive-oriented models aimed at improving gear durability and operational reliability.

ACKNOWLEDGEMENT

For authors T.L and M.S. this work was supported by the Ministry of Science, Technological Development and Innovation, Republic of Serbia, Contract No. 51-03-137/2025-03/200105 and by COST Action CA23155 – A pan-European network of Ocean Tribology (OTC).

REFERENCES

- [1] Ristivojević, M., and Lazović, T.: Influence of kinematic parameters and tooth geometry on gear tooth root load capacity, *Proceedings of the Romanian Academy, Series A*, Vol. 18, No. 2, 2017.
- [2] Farhan Ogaili, A.A., Mohammed, K.A., Jaber, A.A., Al-Ameen, E.S.: Automated Wind Turbines Gearbox Condition Monitoring: A Comparative Study of Machine Learning Techniques Based on Vibration Analysis., *FME Transactions*, Vol. 52, No. 3, pp. 471–485, 2024.
- [3] Chen, T., Zhu, C., Chen, J., and Liu, H.: A review on gear scuffing studies: Theories, experiments and design, *Tribology International*, Vol. 196, p. 109741, 2024.
- [4] Dugic, P., Dugic, M.: Specifications' Influence on Composition and Tribological Characteristics of Industrial Gears Lubricants, *FME Transactions*, Vol. 43, No. 3, pp. 223–227, 2015.
- [5] Höhn, B.R., Michaelis, K.: Influence of oil temperature on gear failures, *Tribology International*, Vol. 37, pp. 103–109, 2004.
- [6] Höhn, B.-R., Michaelis, K., Otto, H.-P.: Influence of immersion depth of dip lubricated gears on power loss, bulk temperature and scuffing load carrying capacity, *International Journal of Mechanics and Materials in Design*, Vol. 4, pp. 145–156, 2008.
- [7] Michalczewski, R., Kalbartszyk, M., Mańkowska-Snopczyńska, A., Osuch-Słomka, E., Piekoszewski, W., Snarski-Adamski, A., Szczerk, M., Tuszyński, W., Wulczyński, J., Wieczorek, A.: The Effect of a Gear Oil on Abrasion, Scuffing, and Pitting of the DLC-Coated 18CrNiMo7-6 Steel, *Coatings*, Vol. 9, No. 1, p. 2, 2019.
- [8] Tuszyński, W., Michalczewski, R., Osuch-Słomka, E., Snarski-Adamski, A., Kalbartszyk, M., Wieczorek, A.N., Nędza, J.: Abrasive Wear, Scuffing and Rolling Contact Fatigue of DLC-Coated 18CrNiMo7-6 Steel Lubricated by a Pure and Contaminated Gear Oil, *Materials*, Vol. 14, No. 22, p. 7086, 2021.
- [9] Wu, J., Wei, P., Liu, G., Chen, D., Zhang, X., Chen, T., Liu, H.: A comprehensive evaluation of DLC coating on gear bending fatigue, contact fatigue, and scuffing performance, *Wear*, Vol. 536–537, p. 205177, 2024.
- [10] Osuch-Słomka, E., Michalczewski, R., Mańkowska-Snopczyńska, A., Kalbartszyk, M., Wieczorek, A.N., and Skołek, E.: Wear Mechanisms of the Working Surface of Gears after Scuffing Tests, *Materials*, Vol. 17, No. 14, p. 3552, 2024.
- [11] Osuch-Słomka, E., Michalczewski, R., Mańkowska-Snopczyńska, A., Gibała, M., Wieczorek, A.N., and Skołek, E.: Influence of Gear Set Loading on Surface Damage Forms for Gear Teeth with DLC Coating, *Coatings*, Vol. 15, No. 7, p. 857, 2025.
- [12] Riggs, M.R., Murthy, N.K., Berkebile, S.P.: Scuffing resistance and starved lubrication behaviour in helicopter gear contacts: Dependence on material, surface finish, and novel lubricants, *Tribology Transactions*, Vol. 60, No. 5, pp. 932-941, 2017.
- [13] Murthy, N.K., Berkebile, S.P., Rai, A.K., Hille, E., Ewin, J.: Effects of ionic liquid additive concentration on scuffing and wear in oil-starved EHL contacts, *Tribology Transactions*, Vol. 61, No. 6, pp. 1117-1130, 2018.
- [14] Xue, J., Li, W., Quin, C.: The scuffing load capacity of involute spur gear systems based on dynamic load and transient thermal elastohydrodynamic lubrication, *Tribology International*, Vol. 79, pp. 74–83, 2014.
- [15] Chang, L., Jeng, Y.-R., and Yu, Q.: Parametric analysis of rolling-sliding line contacts under boundary and near boundary lubrication conditions, *Tribology Transactions*, Vol. 59, pp. 119–127, 2016.
- [16] Wink, C.H.: Predicted scuffing risk to spur and helical gears in commercial vehicle transmissions, *Gear Technology*, pp. 82-86, 2012.
- [17] McCormick, M.: The risk of scuffing, a non-fatigue-based failure mode, can be reduced via isotropic superfinishing, *Gear Solutions*, 0916, pp. 22-23, 2016.
- [18] Pan, A.-X., Wen, C., Wang, H., Tao, P., Liu, X., Gong, Y., Yang, Z.-G.: Failure Analysis of Gear on Rail Transit, *Materials*, Vol. 18, No. 20, p. 4773, 2025.
- [19] Pei, X., Pu, W., Yang, J.: Numerical simulation of defective gear transmission under mixed EHL conditions, *Engineering Failure Analysis*, Vol. 127, p. 105525, 2021.
- [20] Pei, X., Nie, J., Guo, H., Li, S., Zuo, Y.: An involute gear pair meshing stiffness model considering time-varying friction under mixed lubrication,

[21] Castro, J., Seabra, J.: Scuffing and lubricant film breakdown in FZG gears Part I. Analytical and experimental approach, *Wear*, Vol. 215, No. 1, pp. 104–113, 1998.

[22] Castro, J., Seabra, J.: Scuffing and lubricant film breakdown in FZG gears Part II. New PV scuffing criteria, lubricant and temperature dependent, *Wear*, Vol. 215, No. 1, pp. 114–122, 1998.

[23] Castro, J., Seabra, J.: Global and local analysis of gear scuffing tests using a mixed film lubrication model, *Tribology International*, Vol. 41, No. 4, pp. 244–255, 2008.

[24] Castro, J., Seabra, J.: Gear scuffing: power dissipation and mass temperature, *Proceedings of the VIII Iberian Conference on Tribology (Ibertrib 2015)*, pp. 127–134, 2015.

[25] Chen, T., Zhu, C., Liu, H., Ma, K., Zhang, W.: The PVT limit for gear scuffing assessment, *Wear*, Vol. 558–559, p. 205557, 2024.

[26] Zheng, X.-Q., Hui, J.-H., Lan, H.-Q.: Effect of Gear Body Temperature on the Dynamic Characteristics of Spiral Bevel Gears, *Lubricants*, Vol. 13, No. 2, p. 82, 2025.

[27] Pei, X., Huang, L., Pu, W., Wei, P.: Dynamical wear prediction along meshing path in mixed lubrication of spiral bevel gears, *Advances in Mechanical Engineering*, Vol. 12, No. 9, p. 1687814020958236, 2020.

[28] Bai, B., Mao, R., Guo, W., Mao, S.: Research on Calculation and Optimization Methods for Tooth Flash Temperature and Meshing Power Loss of the Gear System in Drum Shearer, *Applied Sciences*, Vol. 14, No. 12, p. 5222, 2024.

[29] Castro, J., Seabra, J.: Influence of mass temperature on gear scuffing, *Tribology International*, Vol. 119, pp. 27–37, 2018.

[30] Cai, Z.-J., Zheng, X.-Q., Lan, H.-Q., Wang, L.-N., Yang, S.-W., Shen, R.: Predictive Model for Scuffing Temperature Field Rise of Spiral Bevel Gears under Different Machining Conditions, *Lubricants*, Vol. 12, No. 10, p. 354, 2024.

[31] Bai, B., Li, X., Guo, W., Mao, S.: Effect of Geometric Parameters of High-Speed Helical Gears on Friction Flash Temperature and Scuffing Load Capacity in Electric Vehicles, *Applied Sciences*, Vol. 14, No. 22, p. 10326, 2024.

[32] Vereš, M., Nemčeková, M., Marinković, A.: Tooth flanks scoring resistance of non-involute teeth profiles in plane toothed cylindrical gears, *FME Transactions*, Vol. 37, No. 2, pp. 103–106, 2009.

[33] Wen, J., Zhou, Y., Tang, J., Dai, Y.: An Effective Analytical Approach to Predicting the Surface Contact Temperature of the Face Gear Drives, *Mathematics*, Vol. 11, No. 14, 2023.

[34] ISO 6336-21:2017, Calculation of load capacity of spur and helical gears—Calculation of scuffing load capacity—Integral temperature method: International Organization for Standardization, 2017.

[35] DIN 3990: Tragfähigkeitsberechnung von Stirnrädern—T4 Berechnung der Fresstragfähigkeit: Deutsches Institut für Normung, 1987.

[36] Marinković, A., Sedak, M., Lazović, T., Rosić, M.: Structural optimisation of planetary gearbox components, *FME Transactions*, Vol. 53, No. 1, pp. 74–84, 2025.

[37] Rackov, M., Vereš, M., Čavić, M., Penčić, M., Kanović, Ž., Kuzmanović, S., Knežević, I.: Optimization of HCR Gearing Geometry from a Scuffing Point of View, *Advanced Gear Engineering*, Springer, pp. 365–392, 2017.

[38] Ganti, V., Dewangan, Y., Arvariya, S., adhavan, S.: Influence of Micro-Geometry on Gear Scuffing, SAE Technical Paper, p. 2015-26-0187, 2015.

[39] Chen, J., Zhu, C., Wei, P., Zeng, P., Wang, B., Chen, T., Liu, H.: Experimental study on high-speed aviation gear scuffing based on tooth profile and surface treatment improvements, *Tribology Transactions*, Vol. 67, No. 2, pp. 280–293, 2024.

[40] Shi, Z., Liu, Y., Zavala, F., Xu, H., and Reinhart, T.: Multi-Objective Optimization of Multi-Stage Gear Transmission Considering Scuffing Risks, *International Design Engineering Technical Conferences and Computers and Information in Engineering Conference*, American Society of Mechanical Engineers, p. V010T10A007, 2024.

[41] Dixit, Y., Kulkarni, M.S.: Multi-objective optimization with solution ranking for design of spur gear pair considering multiple failure modes, *Tribology International*, Vol. 180, p. 108284, 2023.

[42] Kumar, A., Ramkumar, P., Shankar, K.: Multi-objective 3-stage wind turbine gearbox (WTG) with tribological constraint, *Mechanics Based Design of Structures and Machines*, Vol. 52, No. 8, pp. 5263–5289, 2024.

[43] Bußkamp, P., Jacobs, G., Röder, J.: Multiobjective wind turbine gearbox design optimization to reduce component damage risk during grid faults, *Fortschung im Ingenieurwesen*, Vol. 89, No. 1, pp. 1–10, 2025.

[44] Sedak, M., Rosić, B.: Multi-objective optimization of planetary gearbox with adaptive hybrid particle swarm differential evolution algorithm, *Applied Sciences*, Vol. 11, No. 3, p. 1107, 2021.

[45] Wang, Y., Tang, W., Chen, Y., Wang, T., Li, G., Ball, A.D.: Investigation into the meshing friction heat generation and transient thermal characteristics of spiral bevel gears, *Applied Thermal Engineering*, Vol. 119, pp. 245–253, 2017.

[46] Lyu, B., Meng, X., Zhang, R., and Wen, C.: A deterministic contact evolution and scuffing failure analysis considering lubrication deterioration due to temperature rise under heavy loads, *Engineering Failure Analysis*, Vol. 123, p. 105276, 2021.

[47] Ognjanovic, M.: Failure Probability of Gear Teeth Wear, *Fracture of Nano and Engineering Materials*

and Structures: Proceedings of the 16th European Conference of Fracture, Alexandroupolis, Greece, July 3–7, 2006, Springer, pp. 1059–1060, 2006.

[48] Patil, M., Ramkumar, P., Shankar, K.: Multi-objective optimization of spur gearbox with inclusion of tribological aspects, *Journal of Friction and Wear*, Vol. 38, No. 6, pp. 430–436, 2017.

[49] Patil, M., Ramkumar, P., Krishnapillai, S.: Multi-objective optimization of two stage spur gearbox using NSGA-II, SAE Technical Paper, 2017-28-1939, 2017.

[50] Patil, M., Ramkumar, P., Shankar, K.: Multi-objective optimization of the two-stage helical gearbox with tribological constraints, *Mechanism and Machine Theory*, Vol. 138, pp. 38–57, 2019.

[51] International Organization for Standardization: ISO 10825:1995 – Gears – Wear and damage to gear teeth – Terminology, Geneva, Switzerland, 1995.

[52] International Organization for Standardization: ISO 10825-1:2022 – Gears – Wear and damage to gear teeth – Part 1: Nomenclature and characteristics, Geneva, Switzerland, 2022.

[53] International Organization for Standardization: ISO/TR 10825-2:2022 – Gears – Wear and damage to gear teeth – Part 2: Supplementary information, Geneva, Switzerland, 2022.

[54] Dimić, A., Vencl, A., Ristivojević, M., Mitrović, R., Mišković, Ž., Milivojević, A.: Influence of the running-in process on the working ability of contact surfaces in lubricated sliding conditions, *Proceedings of the Institution of Mechanical Engineers, Part J: Journal of Engineering Tribology*, Vol. 236, No. 4, pp. 691–700, 2022.

[55] Dimić, A.R., Ristivojević, M.R., Kolarević, N.M., Mišković, Ž.Z., Sedak, M.I., Djordjević, B.R.: Influence of the Involute Gear Teeth Profile Shape and Running-In on Surface Load Capacity of Cylindrical Gear Pairs, *Tribology Transactions*, Vol. 68, No. 4, pp. 959–973, 2025.

[56] Naunheimer, H., Bertsche, B., Ryborz, J., Nowak, W.: *Automotive Transmissions*, Springer-Verlag, Berlin Heidelberg, 2011.

[57] International Organization for Standardization: ISO 6336-3: Calculation of load capacity of spur and helical gears—Part 3: Calculation of tooth bending strength, Geneva, Switzerland, 2006.

[58] Osakue, E.E., Anetor, L.: Estimating Beam Strength of Metallic Gear Materials, *FME Transactions*, Vol. 50, No. 4, pp. 587–606, 2022.

[59] Osakue, E.E., Anetor, L., Harris, K.: A parametric study of frictional load influence in spur gear bending resistance, *FME Transactions*, Vol. 48, No. 2, pp. 294–306, 2020.

[60] Osakue, E.E., Anetor, L.: Design of Straight Bevel Gear for Pitting Resistance, *FME Transactions*, Vol. 46, No. 2, pp. 194–204, 2018.

[61] International Organization for Standardization: ISO 6336-2: Calculation of load capacity of spur and helical gears—Part 2: Calculation of surface durability (pitting), Geneva, Switzerland, 2006.

[62] International Organization for Standardization: ISO 6336-20:2017, Calculation of load capacity of spur and helical gears—Calculation of scuffing load capacity—Flash temperature method, Geneva, Switzerland, 2017.

[63] Schlecht, B.: *Maschinenelemente*, Pearson Studium, München, Germany, 2010.

[64] Salawu, E., Ajayi, O., Inegbenebor, A., Akinlabi, S., Afolalu, S., Aroyinbo, A.: Material Selection and Processing Techniques: Crucial Factors for Gear Engineering, IOP Conference Series: Materials Science and Engineering, IOP Publishing, p. 012114, 2021.

[65] Chen, T., Wei, P., Zhu, C., Zeng, P., Li, D., Parker, R., Liu, H.: Experimental investigation of gear scuffing for various tooth surface treatments, *Tribology Transactions*, Vol. 66, No. 1, pp. 35–46, 2023.

[66] Markovic, S.L., Lazovic, T.M.: Technological heredity—A decisive factor for tribological features of regenerated gears, *Engineering Failure Analysis*, Vol. 42, pp. 121–132, 2014.

[67] Nikolić, R.R., Marković, S., Arsić, D., Lazić, V., Hadzima, B., Ulewicz, R.: Influence of different hard-facing procedures on quality of surfaces of regenerated gears, *Production Engineering Archives*, Vol. 27, No. 4, pp. 257–264, 2021.

NOMENCLATURE

$B_{M1,2}$	thermal contact coefficients
C_1	experimental weighting factor
C_2	experimentally determined weighting factor
K	empirical factor
M_{T1T}	pinion torque, in Nm
S_{Smin}	minimum scuffing safety factor
S_{intS}	scuffing safety factor
X_{WrelT}	relative structure factor
X_S	lubrication factor
X_ε	contact ratio factor
b_h	face width, in mm
b_h	face width
c_v	specific heat capacity per unit volume, in N/mm ² K
m	module, in mm
n_p	pinion rotational speed, in rpm
ν_{40}	nominal kinematic viscosity, in mm ² /s
$v_{t1,2}$	tangential velocities of radii 1 and 2, in m/s
w_n	line load in the normal direction, in N/mm
z_p	number of pinion teeth
μ_{mC}	average coefficient of friction
ϑ_0	temperature of the lubricating oil before tooth engagement, in °C
ϑ_{fla}	flash temperature, in °C
ϑ_{flaE}	flash temperature at the pinion's engagement point E, in °C
ϑ_{flaint}	average flash temperature, in °C
ϑ_{int}	integral temperature, in °C
ϑ_{intP}	permissible integral temperature, in °C

ϑ_M	mass temperature of the tooth surface just before loading, in °C
ϑ_M	mass temperature, in °C
ϑ_{MT}	mass temperature depending on the pinion torque, in °C
$\vartheta_{flaintT}$	average flash temperature, in °C
λ_M	heat conductivity, in N/sK

**НУМЕРИЧКА АНАЛИЗА РИЗИКА ОД
СКАФИНГА ЦИЛИНДРИЧНИХ ЗУПЧАНИКА
СА ПРАВИМ ЗУПЦИМА ЗАСНОВАНА НА
КРИТЕРИЈУМУ ИНТЕГРАЛНЕ
ТЕМПЕРАТУРЕ**

М. Бозца, Т. Лазовић, М. Седак, С. Бодзаш

Скафинг зупчаника представља један од главних проблема и значајан технички изазов у конструисању механичких преносника снаге. У овом раду дат је преглед савремених истраживања и практичних

приступа разумевању и спречавању појаве скафинга, ослањајући се на индустријска искуства, доступне стандарде и академска истраживања. Развијен је наменски рачунарски програм у MATLAB окружењу који омогућава систематску анализу утицаја геометријских, радних и параметара подмазивања на локалну температуру у контакту зубаца, температуру зупца и интегралну температуру. Резултати показују да повећање модула, броја зубаца и ширине зупчастог венца позитивно утиче на отпорност према скафингу, док повећани обртни моменат, учестаност обртања и температура уља значајно повећавају ризик од скафинга, који као вид отказа може знатно скратити радни век зупчаника. Примењени модел и спроведена анализа указују да добијени резултати могу представљати основу за развој будућих оптимизационих модела, чији је циљ унапређење поузданости зупчаника и продужење њиховог радног века кроз оправдан избор параметара и побољшање конструкције.